Scale-free models of chromosome structure, dynamics, and mechanics

Simon Grosse-Holz,[1,2,*] Antoine Coulon,[2,3,†] and Leonid Mirny[1,2,‡]

[1] *Department of Physics and Institute for Medical Engineering and Science, Massachusetts Institute of Technology, Cambridge, MA 02143, USA*
[2] *Institut Curie, PSL Research University, Sorbonne Université, CNRS UMR3664, Laboratoire Dynamique du Noyau, 75005 Paris, France*
[3] *Institut Curie, PSL Research University, Sorbonne Université, CNRS UMR168, Laboratoire Physico Chimie Curie, 75005 Paris, France*

(Dated: April 14, 2023)

Scale-free, or fractal, models are prevalent in the study of chromosome structure, dynamics, and mechanics. Recent experiments suggest the existence of scaling relationships; but currently there is no single model consistent with all observed exponents. We present a simple argument characterizing the space of scale-free models for chromosome structure, dynamics, and mechanics and discuss the implications for a consistent treatment. Our framework helps reconciling seemingly contradictory data and identifies specific experimental questions to be addressed in future work.

The nucleus of a eukaryotic cell contains its genetic information in the form of chromatin—a composite polymer of DNA and associated proteins. The physical nature of this polymer, and specifically the local chromosomal context of a given locus, play crucial roles in determining how the information encoded on the DNA is processed [1]. So-called *enhancer* elements for example are thought to activate their target genes by "looping in" and physically contacting the target promoter to initiate transcription [2–4]. How this interaction is regulated between elements that can be separated by millions of base pairs remains an open question [5–7]; in fact, the structure and dynamics of even the "bare" chromatin polymer itself—without additional elements like enhancers and promoters—remain topics of active research [8–10].

Our understanding of the 3D structure of chromosomes has increased dramatically over the last decade, primarily due to experimental techniques like Hi-C [11, 12] (measuring pairwise contacts across the genome) and multiplexed FISH methods [13, 14] (visualizing chromosome conformations in 3D space). Both techniques show that the chromatin fiber adopts a *space-filling* conformation: two loci at a genomic separation s are on average separated in space by a distance $R(s) \sim s^{\frac{1}{3}}$ [8], corresponding to a confining volume $V(s) \sim R^3(s) \sim s$ [15]—thus the term "space-filling". The probability $P(s)$ of finding these two loci in contact is then given by the mean field approximation $P(s) \sim 1/V(s)$ [16]; $P(s) \sim s^{-1}$ was broadly observed in Hi-C experiments across vertebrate chromosome systems [11, 12]. Notably, this space-filling spatial organization is more compact than one would expect for an ideal chain in equilibrium, which should adopt a random walk conformation with $R(s) \sim s^{\frac{1}{2}}$, corresponding to $V(s) \sim s^{\frac{3}{2}}$ and $P(s) \sim s^{-\frac{3}{2}}$ [17].

The study of chromosome dynamics has not seen a breakthrough comparable to Hi-C yet and is therefore more heterogeneous. One main mode of investigation is fluorescent labelling and tracking of individual genomic loci in live cells, allowing for characterization of the particles' motion by the Mean Squared Displacement (MSD)

$$\mathrm{MSD}(\Delta t) := \left\langle \left(x(t+\Delta t) - x(t)\right)^2 \right\rangle \sim (\Delta t)^{\mu} \ .$$

While a freely diffusive particle would exhibit a linear MSD curve ($\mu = 1$), a chromosomal locus (i.e. point on a long polymer) is expected to move subdiffusively ($\mu < 1$) due to the chain connectivity. Indeed, experiments show $\mu \approx 0.5-0.6$ in eukaryotic cells [18, 19]. Notably—and in contrast to the spatial structure—this is consistent with an ideal chain ($R(s) \sim s^{\frac{1}{2}}$, $P(s) \sim s^{-\frac{3}{2}}$), for which the Rouse polymer model predicts $\mu = \frac{1}{2}$ [20, 21].

Taking an orthogonal angle on the question of chromatin dynamics, the present authors, together with others, recently developed an experimental system to measure the force response of a single genomic locus [22]. In response to a constant force switched on at $t = 0$ the locus displaced as $x(t; f) \sim t^{0.5}$, consistent with the same (Rouse) model for polymer dynamics that predicted the MSD scaling $\mu = 0.5$—but which is inconsistent with the structure $R(s) \sim s^{\frac{1}{3}}$ of real chromatin.

A model consistent with the space-filling structure of real chromatin is the *fractal globule*, which describes crumpling of the chain due to topological constraints [23]. This, however, predicts an MSD scaling of $\mu = \frac{2}{5}$ [24], markedly lower than the $\mu \approx 0.5-0.6$ observed in experiments. Within the context of commonly used polymer models for chromatin, we are thus left with two mutually contradictory observations: a fractal globule would reproduce the compact structure, but with slower dynamics [25]; the fast dynamics are consistent with the Rouse model, but that assumes an unrealistically open, equilibrium conformation. Does this point to some fundamental inconsistency in structural vs. dynamical observations, or is it simply that both models are wrong? If so, how can we reconcile all observations?

Chromosome structure and organization spans multiple orders of magnitude: from single nucleosomes (∼11 nm) to whole nuclei (∼2–20 µm). As such, *scale-free* models—such as Rouse or fractal globule—constitute

useful null models for the description of chromosomes. Indeed, all the observables mentioned above—contact probability $P(s)$, spatial separation $R(s)$, $\mathrm{MSD}(\Delta t)$, force response $x(t;f)$—are expected to exhibit scaling behavior (read: are powerlaws), exactly because of this scale-free nature of the null model. The point we aim to highlight with this letter is that within the context of scale-free models, not only are these observables governed by powerlaws, but their exponents also have to satisfy hyperscaling relations that are a direct consequence of the scale-free assumption. These relations enable an informed discussion of the mismatch between structure, dynamics, and mechanics highlighted above; awareness of these relations is lacking in the literature [26].

Let us assume we have a scale-free model for chromatin structure, dynamics, and mechanics. Such a model should predict the behavior of the observables outlined in the introduction and because of the absence of finite length scales we expect to find powerlaws. Explicitly, we assume the forms

$$R(s) = Gs^{\nu} \tag{1}$$

for the spatial distance between two loci at a genomic separation s;

$$\mathrm{MSD}(\Delta t) = \Gamma\,(\Delta t)^{\mu} \tag{2}$$

for the MSD of a single genomic locus; and

$$x(t;f) = Af^{\psi}t^{\rho} \tag{3}$$

for displacement in response to a constant force f switched on at time $t = 0$ (red, teal, and orange in fig. 1). Note how the equations concerning dynamics and force response consider only a single locus, while the structural scaling refers to a finite stretch of chromatin. To bridge this gap and connect structure and dynamics, we consider the whole-coil diffusion of a finite and isolated stretch of chromatin. Over timescales longer than the internal relaxation time, we expect this coil to diffuse like a free particle, quantified by an MSD of the form

$$\mathrm{MSD}_{\mathrm{coil}}(\Delta t; s) = Ds^{-\delta}\,(\Delta t)^{\alpha} \tag{4}$$

(blue in fig. 1). Since we expect a free coil to undergo normal diffusion, $\alpha = 1$ seems like the most natural choice; however, allowing $\alpha < 1$ incorporates the possibility of a viscoelastic solvent, such that even a free tracer particle would undergo subdiffusion—which has been observed for the nucleoplasm, though estimates for α vary broadly ($\alpha \approx 0.5-1$) [27–29]. The exponent δ can be understood as incorporating long-range spatial interactions of different loci on the polymer. For a freely draining chain (such as the Rouse model), monomers are independent from each other; whole-coil diffusivity is thus simply inversely proportional to chain length, yielding $\delta = 1$. The Zimm

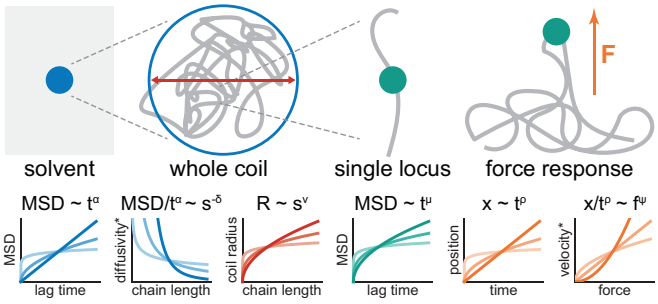

FIG. 1. Summary of the exponents considered in the text and what part of the system they relate to. Left to right: α controls the viscoelasticity of the solvent, i.e. the MSD of a free tracer particle. Considering an isolated polymer coil as such a tracer particle, δ governs the dependence of its (anomalous) diffusivity on the chain length; ν gives the scaling of the physical radius of the coil. The motion of individual loci within the coil is characterized by μ. Upon application of an external force, such loci exhibit a powerlaw response with exponent ρ; the (fractional) velocity of this response is force dependent, as indicated by ψ. Colors indicate which constitutive relation an exponent is associated with: red for eq. (1), teal for eq. (2), orange for eq. (3), and blue for eq. (4).
*: "anomalous diffusivity" if $\alpha \neq 1$
"fractional velocity" if $\rho \neq 1$.

model [21], in contrast, incorporates hydrodynamic interactions between the loci, which results in a hydrodynamic radius $R_{\mathrm{hydro}} \sim R(s)$. $\mathrm{MSD}_{\mathrm{coil}} \sim R_{\mathrm{hydro}}^{-1}$ then implies $\delta = \nu$.

The observables described by eqs. (1) to (4) all have units of length. But we assume that the underlying model itself does not have any finite length scale; this assumption would be inconsistent, if we could construct such a finite length scale from the constants in the model, i.e. from the prefactors in eqs. (1) to (4) and the thermal energy $k_{\mathrm{B}}T$. Their respective dimensions are

$$[k_{\mathrm{B}}T] = LF\,, \qquad [G] = LS^{-\nu}\,, \qquad [\Gamma] = L^2T^{-\mu}\,,$$
$$[A] = LF^{-\psi}T^{-\rho}\,, \qquad [D] = L^2S^{\delta}T^{-\alpha}\,,$$

where we use the symbols L, F, S, T to denote length, force, genomic distance, and time, respectively.

A quantity

$$X := (k_{\mathrm{B}}T)^a\, G^b \Gamma^c A^d D^e \tag{5}$$

now has units

$$[X] = L^{a+b+2c+d+2e} F^{a-\psi d} S^{-\nu b+\delta e} T^{-\mu c-\rho d-\alpha e}\,;$$

setting $[X] = L$—attempting to construct a length scale—gives a system of four equations for the five variables a, b, c, d, e. Elementary substitutions reduce this system to one equation for two variables,

$$\left(1 + \frac{2\nu}{\delta} - \frac{2\alpha\nu}{\delta\mu}\right) b + \left(1 + \psi - \frac{2\rho}{\mu}\right) d = 1\,, \tag{6}$$

Organism	μ	ν	Ref.	Notes
H. sapiens				
HCT-116	-	0.3-0.4[a]	[35]	ΔRad21
	-	0.3-0.4[b]	[14]	
HeLa	0.5	-	[34]	Telomeric probes
U2OS	0.55	-	[34]	Telomeric probes
MF	0.7	-	[34]	Telomeric probes
M. musculus				
mESC	0.5[c]	-	[18]	WT and ΔRAD21
	0.6[c]	-	[19]	WT and ΔRAD21
	-	0.33-0.4[a]	[36]	ΔRAD21
	-	0.15-0.4[b]	[8]	
hepatocytes	-	0.4[a]	[37]	ΔNIPBL
3T3	0.4	-	[34]	Telomeric probes
D. melanogaster	0.58[c]	0.31[c]	[26]	μ and ν determined in same system
S. cerevisiae	-	0.5[a]	[38]	
	0.5	-	[39]	
E. coli	0.4	-	[40]	
Caulobacter	0.4	-	[40]	

[a] from Hi-C contact probability $P(s) \sim s^{-3\nu}$ [16]
[b] direct measurement from multiplexed FISH
[c] two-locus live-cell measurement

TABLE I. Measured scalings for $\mathrm{MSD}(\Delta t) \sim (\Delta t)^{\mu}$ and $R(s) \sim s^{\nu}$. Chromosome structure is frequently not strictly fractal due to loop extrusion; therefore we here focus on experiments where loop extruding factors (Rad21, a component of the cohesin complex) or their loaders (Nipbl) were acutely degraded, where possible. This overview is not exhaustive.

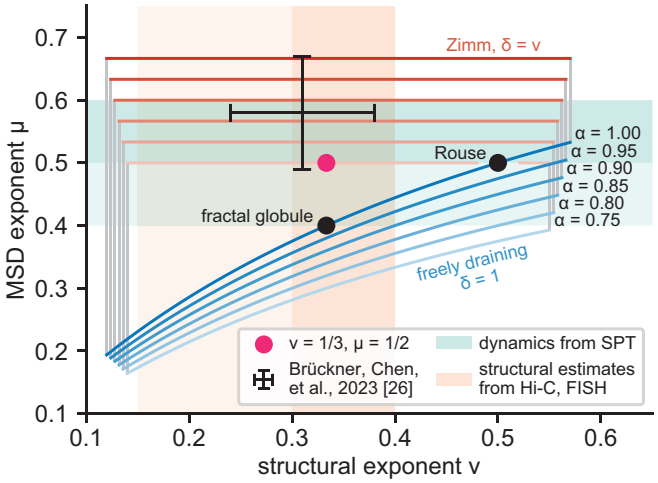

FIG. 2. Experimental results in the context of eq. (7). Shaded regions are consistent with experimental determinations of structure ν (orange; directly from chromosome tracing or inferred from Hi-C, the latter densely shaded) or dynamics μ (green; from SPT; dense shade indicates eukaryotic estimate $\mu \approx 0.5 - 0.6$, light shade extends to bacterial estimate $\mu \approx 0.4$) respectively. Black error bars indicate estimate from [26]. Red circle marks $\nu = 0.33$, $\mu = 0.5$, which serves as example for discussion in the main text. Outlines show theoretically plausible regions (eq. (7)) for different α, as indicated. The top (red) edge of these regions is given by the Zimm condition $\delta = \nu$, while the bottom (blue) edge is given by the freely draining chain ($\delta = 1$); the points inbetween correspond to $\nu < \delta < 1$. Horizontal cutoffs (gray lines) are chosen for visual appeal. Common polymer models: Rouse chain and fractal globule are indicated as black circles; both are instances of a freely draining chain with $\alpha = 1$ (blue curve).

which has a one-parameter family of solutions (b, d)—unless both terms in brackets vanish. The scale-free assumption is thus only self-consistent if the exponents obey the two constraints

$$\frac{2\nu\alpha}{2\nu+\delta} = \mu = \frac{2\rho}{1+\psi}\,. \tag{7}$$

These two constraints ensure that both brackets in eq. (6) vanish, thus preventing the emergence of a finite length scale $[X] = L$. The first relation has been reported previously, in the special cases $\alpha = 1$, $\delta = 1$ [24, 30]; $\nu = \frac{1}{2}$, $\delta = 1$ [31]; and $\delta = 1$ [32]. The second relation connecting dynamics and force-response is satisfied explicitly by the Rouse model [22, 33], but has not been studied in generality.

Consider the force response experiments of [22], where we determined $\rho \approx 0.5$, $\psi \approx 1$, and $\mu \approx 0.5$, fully consistent with eq. (7). Notably, just the linear force response ($\psi = 1$) suffices to predict $\rho = \mu$; our measurement of the force response exponent $\rho \approx 0.5$ can thus be interpreted as an independent validation of earlier experiments finding $\mu \approx 0.5$ [34].

The first relation in eq. (7) connects the structural and dynamical scalings ν and μ, both of which have been investigated in various experimental systems (see table I). While specifically yeast seems consistent with the Rouse expectations $\mu = 0.5$, $\nu = 0.5$, and $\alpha = 1$ [41], multicellular eukaryotes like fruit fly, mouse, or human, seem to behave differently. For the purpose of this discussion, let us consider the case $\mu = 0.5$, $\nu = 0.33$ (fig. 2); this seems consistent with best estimates, but is of course an idealization of the experimental situation. Importantly, eq. (7) holds true for any value of these exponents. As outlined in the introduction, $\mu = 0.5$ matches our expectations from the Rouse model, while $\nu = 0.33$ indicates a fractal globule; to the best of our knowledge, there is currently no consistent model reproducing both. Reformulating the first relation in eq. (7) as

$$\delta = 2\nu\left(\frac{\alpha}{\mu} - 1\right) \tag{8}$$

shows that we should expect a 1-parameter family of models with different α and δ that exhibit the desired scalings in μ and ν. We discuss a few of these options:

- In a freely draining chain (blue lines in fig. 2), individual monomers are independent, such that $\delta = 1$. This assumption is made in the Rouse model and in [24] for dynamics of the fractal globule. Equation (8) then becomes $\alpha = \frac{5}{4} > 1$, i.e. we would

need a medium in which free tracers undergo *superdiffusion*. This appears unrealistic for the nucleoplasm. While it might in principle be achieved by energy dependent processes like transcription or loop extrusion, we will not further pursue this point here.

- Including hydrodynamic interactions between different monomers amounts to $\delta = \nu$, such that $\mu = \frac{2}{3}\alpha$ independent of ν (red lines in fig. 2). This would allow matching $\mu \approx 0.5$ by tuning $\alpha \approx 0.75$. While this is within current estimates for nucleoplasm viscosity, these estimates scatter quite broadly ($\alpha \approx 0.5 - 1$), such that this consistency statement is rather weak. Furthermore, due to crowding we should expect hydrodynamic interactions to be screened in the nucleus [42, 43], such that $\delta = \nu$ appears questionable in the first place.

- Between the two canonical values of $\delta = 1$ (freely draining chain) and $\delta = \nu$ (hydrodynamic interactions), it is conceivable that chromatin loci in the nucleus do exhibit some (effective) long-range interaction with $\nu < \delta < 1$. In a purely viscous nucleoplasm ($\alpha = 1$), eq. (8) would then imply $\delta = 2\nu = \frac{2}{3}$, i.e. a whole-coil hydrodynamic radius scaling as $R_{\mathrm{hydro}} \sim R^2(s)$ (cf. discussion below eq. (4)). While we are currently not aware of a physical model producing this behavior, this is an interesting possibility that certainly warrants further investigation.

Experimentally, there are two avenues to further narrow down the above 1-parameter family to a single, scale-free null model of chromatin in the nucleus: measuring α or δ. Observation of free particle diffusion in the nucleus has so far yielded conflicting results as to the viscoelastic properties of the nucleoplasm: while [28] report $\alpha = 0.5 - 0.6$, [44] measure $\alpha \approx 0.75$ in yeast; [29, 45] find normal diffusion $\alpha = 1$ on large scales (relative to multimeric GFP tracers), with intermediate behavior strongly probe dependent; most recently, [41] reported $\alpha \approx 0.9$ in yeast and $\alpha \approx 0.86$ in mammalian (hPNE) cells. Consensus about nucleoplasm viscosity is thus outstanding. Furthermore, the material whose viscoelasticity is probed here is a solution containing chromatin, which presumably contributes some (if not all) of the observed elastic response; it is thus even unclear what these results would imply for solvent viscoelasticity when modelling chromatin explicitly. We thus suggest that measuring δ (long-range interactions) instead of α (medium viscoelasticity) provides an orthogonal avenue towards a consensus model. Such measurements would require observing the diffusion of free chromatin chains (e.g. nucleosome arrays) of different length in the nucleus, which is feasible with current techniques. A major challenge in such experiments would be to ensure that the probes still obey the same structural scaling ν as the rest of the genome. Early experimental work found $\delta \approx 0.72$ for naked DNA in aqueous solution [46]; we are not aware of similar measurements for chromatinized DNA inside the nucleus.

Our derivation of the exponent relations (7) strongly relied on the absence of finite length scales; of course, no real system is truly scale-free. So what would be implied by experimental data contradicting eq. (7)? First of all, it would simply mean that those data are not well approximated by a single, consistent, scale-free model. It then stands to reason that a more detailed model is required, which will most likely not predict powerlaws for the observables under study in the first place (in which case there are of course also no exponent relations to be satisfied). If any of the observables does indeed exhibit manifestly powerlaw scaling (a claim that is generally quite hard to justify rigorously [47]), the underlying reason might be quite interesting and should be investigated in detail. From a pragmatic point of view, eq. (7) might thus be interpreted simply as a check on the appropriateness of powerlaw fits to multiple observables.

To obtain the connection between unperturbed dynamics and response to an external force, we included the thermal energy $k_{\mathrm{B}}T$ in the set of model constants, because we assume the unperturbed dynamics to be driven by thermal fluctuations. This does not immediately imply an assumption about thermal equilibrium: $k_{\mathrm{B}}T$ in our treatment does not necessarily have to correspond to physical temperature, but should just be some energy scale of the fluctuations. However, many active processes act over a finite length scale, such that in presence of active fluctuations, the scale-free assumption might be questionable. In fact, assuming $T = 37\,^{\circ}\mathrm{C}$ (the physical temperature in the incubation chamber), we found good agreement between MSD and force response in our earlier work [22], suggesting that chromosome fluctuations are indeed largely driven by thermal noise.

We presented a streamlined version of the argument leading to eq. (7), tailored towards the application to polymer structure, dynamics, and mechanics; a more systematic approach to the dimensional analysis is given in the Supplementary Material. Furthermore, the approach through dimensional analysis is of course nothing but a reformulation of the more classical approach based on the consideration of a finite subchain, as given e.g. in [24] for the freely draining chain; we provide that reformulation as appendix.

Acknowledgements. — We are grateful for productive discussions with many colleagues, including Vittore Scolari, Kirill Polovnikov, and members of the Mirny and Coulon groups; Mikhail Tamm; and Jean-François Joanny. Françoise Brochart-Wyart and her work provided valuable inspiration. This work received funding from the Centre National de la Recherche Scientifique (CNRS), the Institut Curie, the European Research Council (ERC) under the European Union's Hori-

zon 2020 research and innovation program (grant agreement 757956), the LabEx CELL(N)SCALE and the LabEx DEEP (ANR-11-LABX-0038, ANR-11-LABX-0044 and ANR-10-IDEX-0001-02), the Agence Nationale de la Recherche (project CHROMAG, ANR-18-CE12-0023-01; project MechaChrom ANR-22-CE95-0003-01), the National Science Foundation (NSF-ANR: Physics of chromosomes through mechanical perturbations, NSF 2210558), the MIT-France Seed Fund, and the Chaire Blaise Pascal program of Île-de-France. Our figures use Paul Tol's *Vibrant* color scheme [48].

Appendix: Finite subchain. — The argument in the main text is formulated in terms of dimensional analysis to emphasize that it is a necessary conclusion of the scale-free assumption. It is easily reformulated in a more physical language by considering a finite subchain of length $\mathfrak{s}$.

Equation (1) gives the physical size of this subchain as

$$\mathfrak{l} = R(\mathfrak{s}) = G\mathfrak{s}^{\nu} .$$

This allows for two independent definitions of a time scale: by setting $\mathrm{MSD}(\Delta t) = \mathfrak{l}^2$ we find

$$\mathfrak{t} = \left(\frac{G^2}{\Gamma}\right)^{\frac{1}{\mu}} \mathfrak{s}^{\frac{2\nu}{\mu}} ;$$

letting instead $\mathrm{MSD}_{\mathrm{coil}}(\Delta t; s) = \mathfrak{l}^2$ yields

$$\tau = \left(\frac{G^2}{D}\right)^{\frac{1}{\alpha}} \mathfrak{s}^{\frac{2\nu+\delta}{\alpha}} .$$

Physically, both describe the relaxation time scale of the coil and should thus be equal (up to a numerical prefactor). This requires that the exponents on $\mathfrak{s}$ be the same, yielding the first relation in eq. (7).

Similarly, eqs. (2) and (3) and the thermal energy $k_{\mathrm{B}}T$ allow the construction of two orthogonal force scales associated with our subchain, both of which should exhibit the same scaling behavior with $\mathfrak{s}$ (or in this case $\mathfrak{l}$):

$$\mathfrak{f} \equiv \frac{k_{\mathrm{B}}T}{\mathfrak{l}} \overset{!}{\sim} \left(\frac{\mathfrak{l}}{A\mathfrak{t}^{\rho}}\right)^{\frac{1}{\psi}} = \left(\frac{\Gamma^{\frac{\rho}{\mu}}}{A}\right)^{\frac{1}{\psi}} \mathfrak{l}^{\frac{1}{\psi}-\frac{2\rho}{\psi\mu}} .$$

Again equating the exponents (on $\mathfrak{l}$) yields the second relation in eq. (7).

While the formulation in terms of a finite subchain can aid physical intuition, the core argument remains the same: if eq. (7) does not hold, a finite length scale emerges. To see this, consider:

$$q(\mathfrak{s}) := \frac{\tau(\mathfrak{s})}{\mathfrak{t}(\mathfrak{s})} = G^{\frac{2}{\alpha}-\frac{2}{\mu}} D^{-\frac{1}{\alpha}} \Gamma^{\frac{1}{\mu}} \mathfrak{s}^{\frac{2\nu+\delta}{\alpha}-\frac{2\nu}{\mu}} .$$

Since q is a dimensionless ratio, if the scaling with $\mathfrak{s}$ were non-trivial, the combination of constants in front would have units of S to some power, translating to a length scale through eq. (1). Thus, within the framework of scale-free models, any finite scale (length, force, or otherwise) associated with the subchain $\mathfrak{s}$ has to be unique. This is ultimately what drives the scaling argument outlined here.

* sgh256@mit.edu
† antoine.coulon@curie.fr
‡ leonid@mit.edu

[1] B. Alberts, A. Johnson, J. Lewis, D. Morgan, M. Raff, K. Roberts, and P. Walter, *Molecular Biology of the Cell*, 6th ed. (Garland Science, Taylor & Francis Group, LLC, New York, 2015).
[2] B. Doyle, G. Fudenberg, M. Imakaev, and L. A. Mirny, Chromatin Loops as Allosteric Modulators of Enhancer-Promoter Interactions, PLOS Computational Biology **10**, e1003867 (2014).
[3] J. Zuin, G. Roth, Y. Zhan, J. Cramard, J. Redolfi, E. Piskadlo, P. Mach, M. Kryzhanovska, G. Tihanyi, H. Kohler, M. Eder, C. Leemans, B. van Steensel, P. Meister, S. Smallwood, and L. Giorgetti, Nonlinear control of transcription through enhancer–promoter interactions, Nature **604**, 571 (2022).
[4] M. A. Zabidi and A. Stark, Regulatory Enhancer–Core-Promoter Communication via Transcription Factors and Cofactors, Trends in Genetics **32**, 801 (2016).
[5] B. Lim and M. S. Levine, Enhancer-promoter communication: hubs or loops?, Current Opinion in Genetics & Development Genome Architecture and Expression, **67**, 5 (2021).
[6] O. Kyrchanova and P. Georgiev, Mechanisms of Enhancer-Promoter Interactions in Higher Eukaryotes, International Journal of Molecular Sciences **22**, 671 (2021).
[7] C. C. Galouzis and E. E. M. Furlong, Regulating specificity in enhancer–promoter communication, Current Opinion in Cell Biology **75**, 102065 (2022).
[8] Y. Takei, J. Yun, S. Zheng, N. Ollikainen, N. Pierson, J. White, S. Shah, J. Thomassie, S. Suo, C.-H. L. Eng, M. Guttman, G.-C. Yuan, and L. Cai, Integrated spatial genomics reveals global architecture of single nuclei, Nature **590**, 344 (2021).
[9] S. Ide, S. Tamura, and K. Maeshima, Chromatin behavior in living cells: Lessons from single-nucleosome imaging and tracking, BioEssays **44**, 2200043 (2022).
[10] A. Zidovska, D. A. Weitz, and T. J. Mitchison, Micron-scale coherence in interphase chromatin dynamics, Proceedings of the National Academy of Sciences **110**, 15555 (2013).
[11] E. Lieberman-Aiden, N. L. van Berkum, L. Williams, M. Imakaev, T. Ragoczy, A. Telling, I. Amit, B. R. Lajoie, P. J. Sabo, M. O. Dorschner, R. Sandstrom, B. Bernstein, M. A. Bender, M. Groudine, A. Gnirke, J. Stamatoyannopoulos, L. A. Mirny, E. S. Lander, and J. Dekker, Comprehensive Mapping of Long-Range Interactions Reveals Folding Principles of the Human Genome, Science **326**, 289 (2009).
[12] S. S. Rao, M. H. Huntley, N. C. Durand, E. K. Stamenova, I. D. Bochkov, J. T. Robinson, A. L. Sanborn, I. Machol, A. D. Omer, E. S. Lander, and E. L. Aiden, A

3D Map of the Human Genome at Kilobase Resolution Reveals Principles of Chromatin Looping, Cell **159**, 1665 (2014).

[13] S. Wang, J.-H. Su, B. J. Beliveau, B. Bintu, J. R. Moffitt, C.-t. Wu, and X. Zhuang, Spatial organization of chromatin domains and compartments in single chromosomes, Science **353**, 598 (2016).

[14] B. Bintu, L. J. Mateo, J.-H. Su, N. A. Sinnott-Armstrong, M. Parker, S. Kinrot, K. Yamaya, A. N. Boettiger, and X. Zhuang, Super-resolution chromatin tracing reveals domains and cooperative interactions in single cells, Science **362**, eaau1783 (2018).

[15] A. N. Boettiger, B. Bintu, J. R. Moffitt, S. Wang, B. J. Beliveau, G. Fudenberg, M. Imakaev, L. A. Mirny, C.-t. Wu, and X. Zhuang, Super-resolution imaging reveals distinct chromatin folding for different epigenetic states, Nature **529**, 418 (2016), number: 7586 Publisher: Nature Publishing Group.

[16] J. D. Halverson, W. B. Lee, G. S. Grest, A. Y. Grosberg, and K. Kremer, Molecular dynamics simulation study of nonconcatenated ring polymers in a melt. I. Statics, The Journal of Chemical Physics **134**, 204904 (2011).

[17] M. Rubinstein and R. Colby, *Polymer Physics* (OUP Oxford, 2003).

[18] M. Gabriele, H. B. Brandão, S. Grosse-Holz, A. Jha, G. M. Dailey, C. Cattoglio, T.-H. S. Hsieh, L. Mirny, C. Zechner, and A. S. Hansen, Dynamics of CTCF- and cohesin-mediated chromatin looping revealed by live-cell imaging, Science **376**, 496 (2022).

[19] P. Mach, P. I. Kos, Y. Zhan, J. Cramard, S. Gaudin, J. Tünnermann, E. Marchi, J. Eglinger, J. Zuin, M. Kryzhanovska, S. Smallwood, L. Gelman, G. Roth, E. P. Nora, G. Tiana, and L. Giorgetti, Cohesin and CTCF control the dynamics of chromosome folding, Nature Genetics **54**, 1907 (2022).

[20] P. E. Rouse, A Theory of the Linear Viscoelastic Properties of Dilute Solutions of Coiling Polymers, The Journal of Chemical Physics **21**, 1272 (1953).

[21] M. Doi and S. F. Edwards, *The theory of polymer dynamics*, International series of monographs on physics ; 73 (Clarendon Press, Oxford [Oxfordshire, 1988).

[22] V. I. P. Keizer, S. Grosse-Holz, M. Woringer, L. Zambon, K. Aizel, M. Bongaerts, F. Delille, L. Kolar-Znika, V. F. Scolari, S. Hoffmann, E. J. Banigan, L. A. Mirny, M. Dahan, D. Fachinetti, and A. Coulon, Live-cell micromanipulation of a genomic locus reveals interphase chromatin mechanics, Science **377**, 489 (2022).

[23] A. Grosberg, Y. Rabin, S. Havlin, and A. Neer, Crumpled Globule Model of the Three-Dimensional Structure of DNA, Europhysics Letters **23**, 373 (1993).

[24] M. Tamm, L. Nazarov, A. Gavrilov, and A. Chertovich, Anomalous Diffusion in Fractal Globules, Physical Review Letters **114**, 178102 (2015).

[25] "slower" here technically meaning "more recurrent", i.e. a lower *exponent*.

[26] D. B. Brückner, H. Chen, L. Barinov, B. Zoller, and T. Gregor, Stochastic motion and transcriptional dynamics of distal enhancer–promoter pairs on a compacted chromosome (2023), bioRxiv preprint, DOI:10.1101/2023.01.18.524527.

[27] I. Golding and E. C. Cox, Physical Nature of Bacterial Cytoplasm, Physical Review Letters **96**, 098102 (2006).

[28] M. Weiss, Probing the Interior of Living Cells with Fluorescence Correlation Spectroscopy, Annals of the New York Academy of Sciences **1130**, 21 (2008).

[29] M. Baum, F. Erdel, M. Wachsmuth, and K. Rippe, Retrieving the intracellular topology from multi-scale protein mobility mapping in living cells, Nature Communications **5**, 4494 (2014).

[30] P. G. De Gennes, Dynamics of Entangled Polymer Solutions. I. The Rouse Model, Macromolecules **9**, 587 (1976).

[31] S. C. Weber, J. A. Theriot, and A. J. Spakowitz, Subdiffusive motion of a polymer composed of subdiffusive monomers, Physical Review E **82**, 011913 (2010).

[32] K. Polovnikov, M. Gherardi, M. Cosentino-Lagomarsino, and M. Tamm, Fractal Folding and Medium Viscoelasticity Contribute Jointly to Chromosome Dynamics, Physical Review Letters **120**, 088101 (2018).

[33] H. Schiessel, G. Oshanin, and A. Blumen, Dynamics and conformational properties of polyampholytes in external electrical fields, The Journal of Chemical Physics **103**, 5070 (1995).

[34] I. Bronshtein, I. Kanter, E. Kepten, M. Lindner, S. Berezin, Y. Shav-Tal, and Y. Garini, Exploring chromatin organization mechanisms through its dynamic properties, Nucleus **7**, 27 (2016).

[35] S. S. Rao, S.-C. Huang, B. Glenn St Hilaire, J. M. Engreitz, E. M. Perez, K.-R. Kieffer-Kwon, A. L. Sanborn, S. E. Johnstone, G. D. Bascom, I. D. Bochkov, X. Huang, M. S. Shamim, J. Shin, D. Turner, Z. Ye, A. D. Omer, J. T. Robinson, T. Schlick, B. E. Bernstein, R. Casellas, E. S. Lander, and E. L. Aiden, Cohesin Loss Eliminates All Loop Domains, Cell **171**, 305 (2017).

[36] T.-H. S. Hsieh, C. Cattoglio, E. Slobodyanyuk, A. S. Hansen, X. Darzacq, and R. Tjian, Enhancer–promoter interactions and transcription are largely maintained upon acute loss of CTCF, cohesin, WAPL or YY1, Nature Genetics **54**, 1919 (2022).

[37] W. Schwarzer, N. Abdennur, A. Goloborodko, A. Pekowska, G. Fudenberg, Y. Loe-Mie, N. A. Fonseca, W. Huber, C. H. Haering, L. Mirny, and F. Spitz, Two independent modes of chromatin organization revealed by cohesin removal, Nature **551**, 51 (2017).

[38] S. Kim, I. Liachko, D. G. Brickner, K. Cook, W. S. Noble, J. H. Brickner, J. Shendure, and M. J. Dunham, The dynamic three-dimensional organization of the diploid yeast genome, eLife **6**, e23623 (2017).

[39] H. Hajjoul, J. Mathon, H. Ranchon, I. Goiffon, J. Mozziconacci, B. Albert, P. Carrivain, J.-M. Victor, O. Gadal, K. Bystricky, and A. Bancaud, High-throughput chromatin motion tracking in living yeast reveals the flexibility of the fiber throughout the genome, Genome Research **23**, 1829 (2013).

[40] S. C. Weber, A. J. Spakowitz, and J. A. Theriot, Bacterial Chromosomal Loci Move Subdiffusively through a Viscoelastic Cytoplasm, Physical Review Letters **104**, 238102 (2010).

[41] T. Shu, T. Szórádi, G. R. Kidiyoor, Y. Xie, N. L. Herzog, A. Bazley, M. Bonucci, S. Keegan, S. Saxena, F. Ettefa, G. Brittingham, J. Lemiere, D. Fenyö, F. Chang, M. Delarue, and L. J. Holt, nucGEMs probe the biophysical properties of the nucleoplasm (2021), bioRxiv preprint, DOI:10.1101/2021.11.18.469159.

[42] P. G. De Gennes, Dynamics of Entangled Polymer Solutions. II. Inclusion of Hydrodynamic Interactions, Macromolecules **9**, 594 (1976).

[43] J. Skolnick, Perspective: On the importance of hydrodynamic interactions in the subcellular dynamics of macro-

molecules, The Journal of Chemical Physics **145**, 100901 (2016).

[44] I. M. Tolić-Nørrelykke, E.-L. Munteanu, G. Thon, L. Oddershede, and K. Berg-Sørensen, Anomalous Diffusion in Living Yeast Cells, Physical Review Letters **93**, 078102 (2004).

[45] F. Erdel, M. Baum, and K. Rippe, The viscoelastic properties of chromatin and the nucleoplasm revealed by scale-dependent protein mobility, Journal of Physics: Condensed Matter **27**, 064115 (2015).

[46] G. L. Lukacs, P. Haggie, O. Seksek, D. Lechardeur, N. Freedman, and A. S. Verkman, Size-dependent DNA Mobility in Cytoplasm and Nucleus *, Journal of Biological Chemistry **275**, 1625 (2000).

[47] M. P. H. Stumpf and M. A. Porter, Critical Truths About Power Laws, Science **335**, 665 (2012).

[48] P. Tol, Color Schemes and Templates (2023), `https://personal.sron.nl/~pault/`, accessed 2023-04-03.